Corrosion and Its Influence on Strength of Steel Bridge Members

JOHN W. FISHER, BEN T. YEN, AND DAYI WANG

INTRODUCTION

Extensive corrosion damage is often observed in girders, floor beams, and stringers of steel girder bridges and in the truss members and their floor system of truss bridges. The loss of material often results in complete corrosive penetration of the plates or rolled components. Figures 1 to 3 show examples of complete penetration of a built-up hanger, batten plate on a chord and the web of a girder. Significant reductions in cross-section areas are possible as a result of active corrosion cell activity[1].

Severe notches in the flanges can develop, particularly where dirt and debris accumulate and create an active corrosion cell. This type notching will occur in all steel materials. Figures 4 and 5 show corrosion notched flange angles of riveted girder members. In Figure 4, dirt and debris accumulated under a diaphragm, and this provided an active corrosion cell site.

The rusting process of steel (or iron) is two-fold involving the chemical change of iron to iron oxide and secondly the electrical process of current flow. Hence, it is an electrochemical process similar to the conditions that develop in a battery[1,2].

The corrosion battery requires oxygen and an electrolyte. For the corrosion conditions generally observed at bridge members, the electrolyte is a solution in water of salts or other chemical compounds, which are capable of conducting electrical current. The current carrying capacity of the electrolyte is due to the presence of electrically charged particles called ions. Ions are formed by the splitting of salts or caustic chemical dissolved in water into mobile, electrically charged fragments. These electrically charged fragments are present in great numbers, and readily conduct current. Ions cannot carry current under dry conditions, so the presence of water is essential for the corrosion battery to function.

Figure 6 shows a schematic representation of an active corrosion battery. It represents a magnified portion of the steel surface. Tiny adjacent areas act as anode and cathode on and adjacent to the surface where water contains ions and serves as the electrolyte. Gaseous oxygen is dissolved in the electrolyte and is available to the metal surface. As the schematic shows, the external circuit is provided by the electrolyte and the internal circuit by the metal.

As the corrosion battery operates, atoms of metallic iron are converted to iron ions which react with the water and oxygen to form rust. As the iron anode is eaten away, a growing deposit of rust forms. Although the iron cathode is not attacked, it serves as a site for oxygen reaction. This process will continue until all of the iron is converted to rust or until the battery circuit is broken. The perforations and notches shown in Figures 1 to 5 are examples of active corrosion cell activity.

Crevices or pockets exist at the edge of the angles used to connect end connections and flange angles to the girder web. Crevices have a tendency to corrode at a far faster rate than the adjacent flat metal areas. Figure 7 shows a schematic of the corrosion battery that tends to develop at the crevice between the angle and web interface. The essential elements of the corrosion process of oxygen, water and ions must be present. Crevices generally trap dirt, salt and rust, and with water, promote galvanic corrosion with the anode provided by the web at the crevice and with the cathode of the steel adjacent to the crevice. The steel in the crevice is an oxygen starved area, acts as the anode, and becomes corroded. Both the web plate adjacent to the connection and crevices in the connection are anodes. However, the corrosive attack is greatest where the anodic and cathodic regions meet as

shown in Figure 3. When the angles are more flexible, the corrosion cell can extend into the joint.

Pitting corrosion results in an extremely localized electrochemical process that produces local holes. It occurs when a small area of the metal surface becomes anodic to the rest of the surface. An anode will often form at a point where oxide film or paint coating breaks occur, so that the external electrolyte comes in contact with a small area relative to the larger surrounding cathodic area. Mill-scale is a form of iron oxide created during the steel rolling process. It is a hard brittle film that adheres to the steel surface, is fragile, and is subject to cracking and spalling. Mill-scale is also cathodic with respect to the steel surface and can accelerate galvanic corrosion. The failure resulting from painting over mill-scale is shown schematically in Figure 8. When the coating is applied over mill-scale, small bare steel areas may exist. After cracking of the coating occurs, a corrosion battery will be set up and the small bare areas will be subject to attack from the large cathodic areas. As the pitting and rust and dirt build up, it will result in peeling, blistering and rupturing, as was illustrated in Figures 1 and 3. The oxygen concentration cell under the surface deposit and coating creates an accelerated galvanic corrosion reaction. When dirt and debris are not present, pitting can develop at the surface, as illustrated in Figure 9.

The rate of corrosion is related to the aggressiveness of the electrolyte. In industrial and marine atmosphere the rate of pitting penetration can be up to 100 times faster than the general corrosion rate[1].

Under general atmospheric exposure, structural steels experience an average corrosion penetration, as illustrated in Figure 10. This shows a plot developed by Horton in 1965 comparing the corrosion of plain carbon, copper-bearing and Mayari R steel (A588) in the Pittsburgh area[3].

The effects of corrosion on the strength and performance of steel members are the areas of concern. A common assumption is that the net area strength will be governed by yielding. However, the corrosion notch may result in fatigue cracking. Corrosion notches may provide a substantial reduction in fatigue resistance, as was demonstrated in References 4 and 5. Cracks developed in the gross section at the notches with little or no influence of rivet holes.

Figure 11 shows the cracks that developed in the heavily corroded flange angle and web plate of the built-up section from a bridge member. It can be seen that the flange angle crack was not influenced by the rivet holes.

The ultimate strength of the corroded riveted section, and the fatigue resistance of corroded riveted member will be examined from the available experimental data.

FATIGUE STRENGTH OF CORROSION NOTCHED MEMBERS

The corrosion notches shown in Figures 4, 5 and 12, resulted in fatigue cracking, as illustrated in Figures 11 and 13. The fatigue resistance of corrosion notched riveted sections has been examined with full scale tests on riveted members with regions of corrosion reduced flange angle thickness, as was illustrated in Figures 4, 5 and 12[4,5]. In Reference 4, five members with corroded sections failed at a corrosion-reduced section. In Reference 5, three members with corroded sections resulted in fatigue cracking. These test results are summarized in Figure 14. All of the cracks initiated in corrosion notched flange angles of the eight test girders. The degrees of reduction in the flange angle cross-section, however, were quite different and varied from 5 to 40% of the angle leg area. The angle leg thickness reduction was the principal influence on the fatigue strength of the detail. In three cases there was also a reduced width. These effects resulted in significant stress concentration at the corroded section. The stress elevations resulted from the notches on the rough irregular surface. No convenient measure of quantifying this was found. Figure 4 shows the reduced section of beam 1 which lost about 60% of its thickness. Cracking was observed to initiate at multiple sites in the region near the edge of the angle, where the thickness was minimal. No cracking was observed in the corroded region of members when the maximum thick-

ness reduction was less than half the original thickness. In those cases cracks developed at rivet holes.

The most severely corroded angle evaluated in Reference 4 is shown in Figure 5. The angle leg was about 40% corroded away. After cracking developed at the corroded section, this detail was retrofitted by drilling a hole at the crack tip and splicing the section. The crack had propagated to near the mid-depth of the web at the time of retrofit, as can be seen in Figure 11.

The fatigue test data of the corroded flange angles are plotted in Figure 14. The stress range is based on the net section of the corroded section. The stress range at the corroded net section varied from 8.3 ksi (57.2 MPa) to 14.1 ksi (97.2 MPa). Also plotted in Figure 14 are the results of the three girders that developed fatigue cracks at corrosion notches in Ref. 5. These three members were subjected to higher stress range levels at the corrosion "net area." The stress range varied from 12 ksi (82.7 MPa) to 18 ksi (124.1 MPa). All three girders had cover plates, as can be seen in Figs. 12 and 13. One of the girders cracked at the end of a cover plate. The other two girders developed cracks in the cover-plated section where the corrosion notches in the sections were severe.

The mechanism of crack formation in the corroded area proceeded as follows. First, several small cracks formed in the rough surface at the deeper notches close to the flange tip. These cracks coalesced and formed a long, shallow surface crack. This surface crack then propagated through the flange thickness at the tip and became an edge crack. Small cracks continued to form in the corroded surface and coalesced with the edge crack. The crack length measured at the bottom surface of the angle leg always lagged behind the length at the corroded top surface.

The test results plotted in Figure 14 demonstrate that the most severely corroded section provides a fatigue resistance comparable to Category E. Three of the test girders provided fatigue lives bounded by the Categories D and E AASHTO and AREA resistance curves. Those girders with a loss of thickness equal to about 50% of the flange thickness approached the lower bound resistance curve provided by Category C.

STRENGTH OF CORRODED HANGERS

Two hangers with severe corrosion loss (39 to 41%) were removed from the Grand Narrows Bridge in Nova Scotia. This structure had experienced severe and rapid corrosion penetration in a large number of the truss and floor system members. In 1983 it was decided to stop maintaining the structure, because of the possibility of constructing a new structure jointly with the Highway Authority[6]. Inspections were carried out yearly between 1979 and 1987[7]. Extensive pitting and crevice corrosion was observed in most of the bridge members. The structure is in a severe marine environment and experienced an acceleration in pitting corrosion in most of its members, as illustrated in Figures 1 and 2. These local pitting holes quickly enlarged and resulted in complete loss of the outstanding leg in local areas. Figure 15 shows how the ratio of remaining net area to the original net area changed at the corroded region for the period between 1982 and 1987. An examination of samples by CN Rail verified that pitting corrosion had indeed developed. With the aggressive marine atmosphere at Grand Narrows, the rate of pitting penetration can be up to 100 times faster than the general corrosion rate. Hence, unprotected 3/8 in. plate could be perforated in less than three years. The local effect is not quite as severe on the total cross-section, as can be seen in Figure 15.

The hangers were tested to failure in a static test in order to assess the residual strength and evaluate the adequacy of the limit state model.

The test specimens were 20 ft. (6.10 m) long, cut from the lower end of the 30 ft. -8 in. (9.35 m) long hangers. End plates were bolted to the flanges for anchorage and load application. Figure 16 is a photograph of the pin-connections at the ends of the hanger. Thus, the hangers were subjected to axial loads only, without end moments.

The corroded portions of the hangers were placed at the lower end of the test setup to simulate the actual orientation of the hangers in the structure.

Six strain gages were mounted on each specimen near midheight: one gage on each of the angles and two on the web. Also attached to each specimen were four LVDT's for the measurement of overall elongation and elongation of the corroded portion. Both specimens failed by excessive elongation and local cracking of the angles at the corroded region. Figure 17 shows the load-elongation plots from the LVDT data. The overall elongation at maximum load was about 1.75 in. (44.5 mm). At termination of the test, the deformation was about 2 in. (50.8 mm) for the 16 ft. (4.9 m) measurement length of the specimens. Figures 18 and 19 are examples of the cracked flange angles of specimens No. 1 and 2. Testing was continued until the applied load dropped substantially below the maximum load. The maximum applied loads, P_{max}, are listed in Table 1, together with the computed reference forces and the section properties.

At the maximum applied load, strains at some of the gages were close to the yield level. One gage was subjected to very high strain because it was adjacent to the corroded area and sensitive to bending. The hangers were severely corroded in the region just above the floor beam connection. Measurement of remaining thickness of the components indicated a measured net cross-section area, A_{nm}, of 11.3 in.^{2} (7290 mm^2) and 10.8 in.^{2} (6968 mm^2) for hangers No. 1 and 2, respectively (Figure 20). Based on these net areas and the average measured ultimate strength of the hanger components, the predicted ultimate net section tensile strength would be 666 kips (2960 kN) and 610 kips (2711 kN), respectively. The corresponding maximum applied test loads were 638 kips (2836 kN) and 584 kips (2596 kN). These values are compared in Table 1.

The maximum applied loads corresponded to slightly less than the computed ultimate tensile strength. The non-uniform corrosion introduces a "shear lag" effect and reduced capacity by about 5%. The hangers did not fail by sudden fracture but exhibited ductile behavior.

The experiments demonstrated that the corroded section was capable of developing the tensile capacity of the remaining net area. The effect of the corrosion on the member strength and ductility was similar to the behavior of mechanically fastened tension members[8]. The local bending which resulted from the lack of symmetry at the severely corroded sections did not deteriorate the tensile strength a significant amount.

SUMMARY

The effects of significant corrosion loss on the strength and performance of riveted members has been examined by full scale tests on members removed from bridge structures.

It is important to note that in actual structures, cracks are seldom observed at the corrosion notched section until significant loss in the total section has occurred. This appears to result from the fact that the rate of corrosion in actual structures often exceeds the rate for fatigue damage thus preventing the development of cracks. Any local damage from cyclic loading appears to be removed by the ongoing corrosion process. Cracks only form when the corrosion loss becomes extensive and causes a substantial increase in the cyclic stress.

When cracks are initiated at a corrosion notched element, the fatigue tests have demonstrated that the corrosion notch effect can be as severe as Category E of the AASHTO and AREA specifications. The results discussed here indicated that the thickness of the corroded riveted member must be reduced by about 50% before the corrosion notch becomes more severe than the rivet holes. The riveted member then provides a fatigue resistance corresponding to Category C. As the thickness reduction increased beyond 50%, the corrosion notch effect became more severe creating its own fatigue initiated detail. Seldom did the resulting fatigue crack intersect a rivet hole. More often it propagated in the gross section of the riveted member.

The ultimate strength tests on corrosion damaged hangers demonstrated that the hangers were able to resist maximum axial loads about equal to the tensile strength on the net section at the corroded area. Hence, the use of an effective net area using the combined corrosion reductions and the hole pattern permitted a reasonable estimate of the limit state.

Both hanger specimens failed in a duc-

tile manner. The corroded region did not significantly reduce the ductility of the material.

ACKNOWLEDGMENTS

This paper was prepared with the support of the NSF Engineering Research Center, Advanced Technology for Large Structural Systems (ATLSS) at Lehigh University. It draws extensively on experimental work carried out at Fritz Engineering Laboratory under sponsorship of the National Cooperative Highway Research Program and the Federal Highway Administration, Department of Transportation during the 1970-1988 period.

Thanks are also due the Canadian National Railroad for the opportunity to examine and evaluate the behavior and characteristics of bridge structures subject to corrosion deterioration.

REFERENCES

(1) "Failure Analysis and Prevention of Corrosion Failures," pp. 168-204, Metals Handbook, Vol. 10, 8th Ed., 1975.

(2) Dismuke, T. D., Coburn, S. K. and Hirsch, C. M.; HANDBOOK OF CORROSION PROTECTION FOR STEEL PILE STRUCTURES IN MARINE ENVIRONMENTS, AISI PI 072-581-5M-EP, 1981.

(3) Horton, J. B., "The Rusting of Low Alloy Steels in the Atmosphere," Presented at the San Francisco Meeting, AISI, Nov. 18, 1965 (see also Bethlehem Steel Booklet 2385-A).

(4) Out, J. H., Fisher, J. W. and Yen, B. T., FATIGUE STRENGTH OF WEATHERED AND DETERIORATED RIVETED MEMBERS, Final Report DOT/OST/P-34/85/016, U.S. DOT, Oct. 1984.

(5) Fisher, J. W., Yen, B. T., Wang, D. and Mann, J. E., FATIGUE AND FRACTURE EVALUATION FOR RATING RIVETED BRIDGES," NCHRP Report 302, Dec. 1987.

(6) Sweeney, R. A. P., Director Structures Design, C. N. Rail, Personal Correspondence to J. W. Fisher, Jan. 1987.

(7) Oommen, G., Engineer, C. N. Rail, Personal Correspondence to J. W. Fisher, Jan. 13, 1987.

(8) Kulak, G. L., Fisher, J. W. and Struik, J. H. A., GUIDE TO DESIGN CRITERIA FOR BOLTED AND RIVETED JOINTS, John Wiley and Sons, 2nd Ed., 1987.

TABLE 1
CROSS-SECTIONAL AREA AND AXIAL LOADS

		Hanger 1	Hanger 2	
Original	An	18.4	18.4	($in.^2$)
Area	Ag	20.6	20.6	
Measured	Anm	11.3	10.8	
Material	Fu	58.9	56.5	(ksi)
Strength	Fy	33.7	32.9	
Computed	AnmFu	666	610	(kips)
Capacity	AngFy	694	678	
Test	P_{max}	638	584	

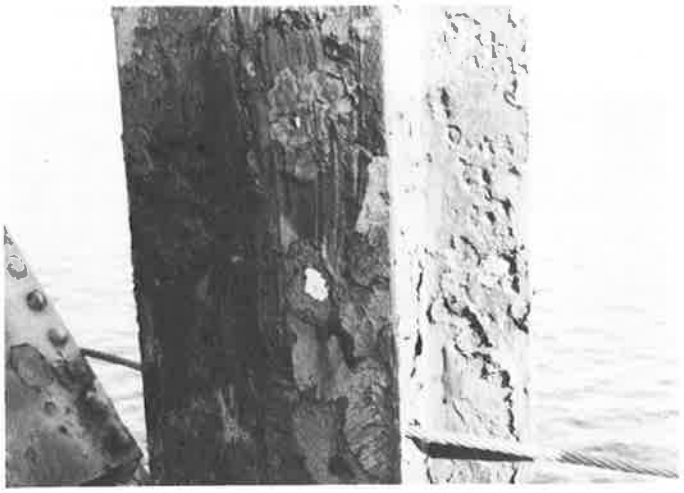

Figure 1 Corrosion Penetration of Riveted Hanger Components

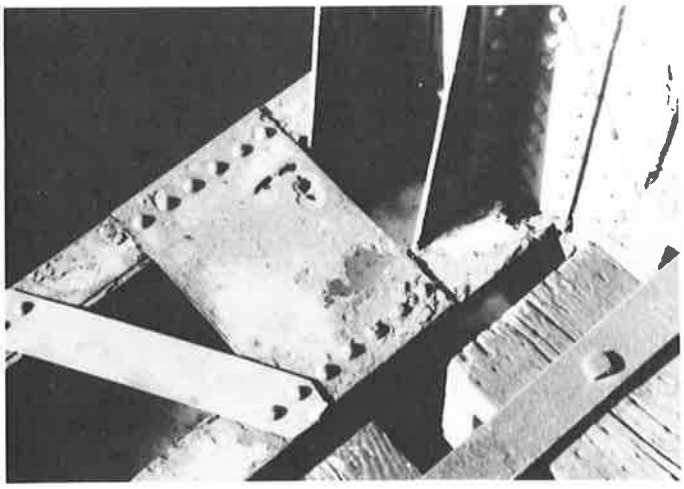

Figure 2 Local Corrosion Penetration of Batten Plate and Chord Components

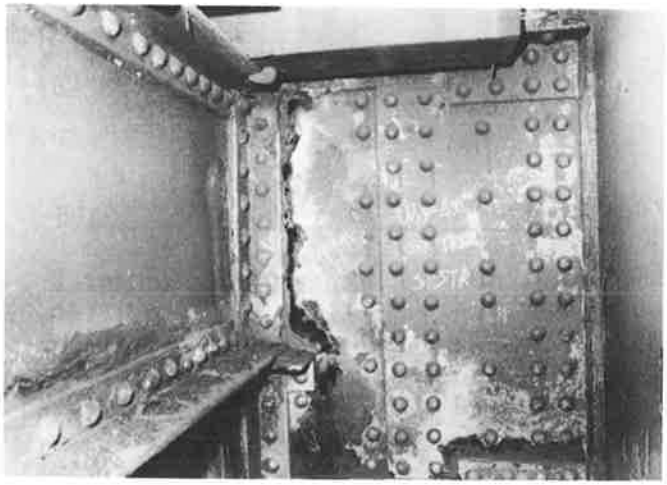

Figure 3 Corroded Web Penetration Along Vertical Angle Legs of Stringer End Connection to Floor Beam

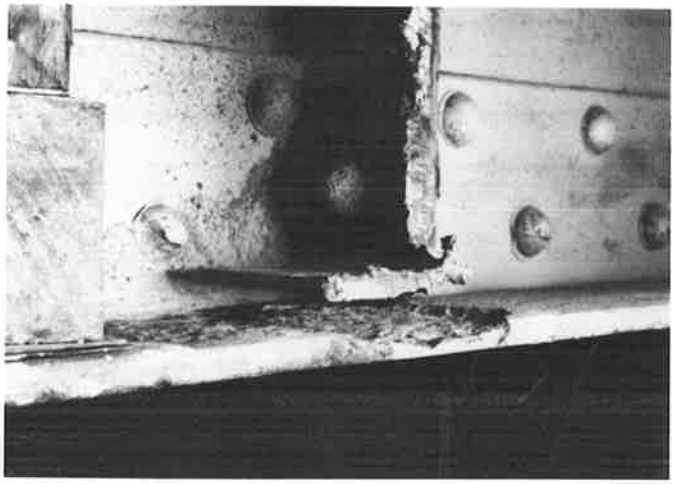

Figure 4 Corrosion Notched Flange Angle Below Diaphragm Where Dirt and Debris Accumulates

Figure 5 Severe Corrosion Notching of Flange Tip

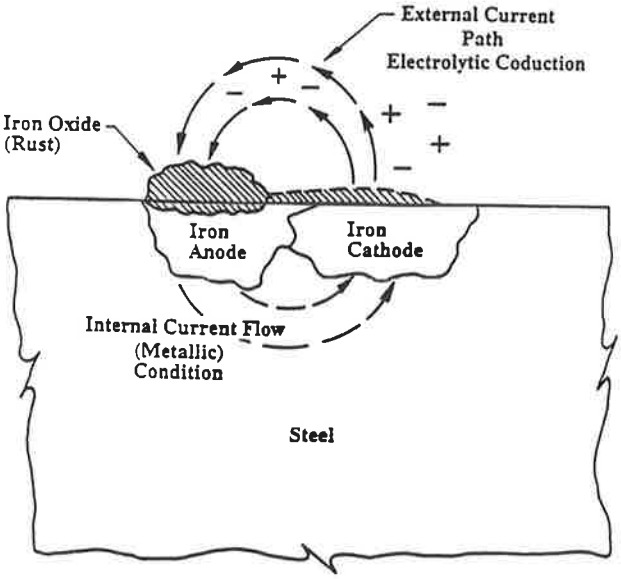

Figure 6 Schematic of Corrosion Cell (Battery)

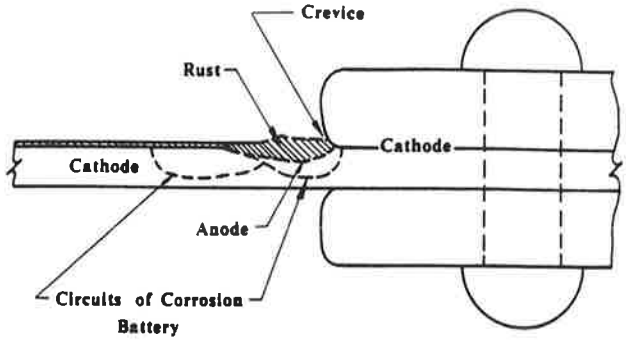

Figure 7 Crevice Corrosion Cell Created at Web-Connection Interface

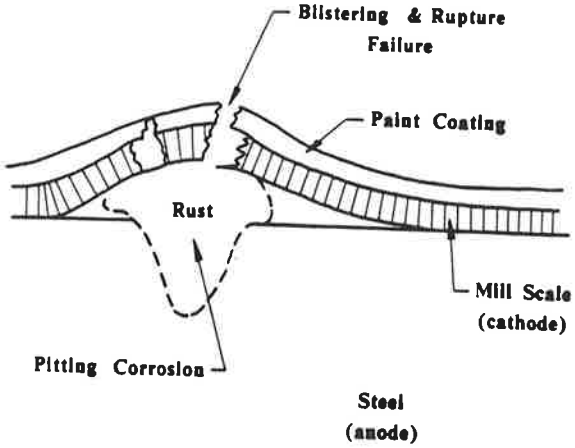

Figure 8 Corrosion Cell at Break in Mill Scale

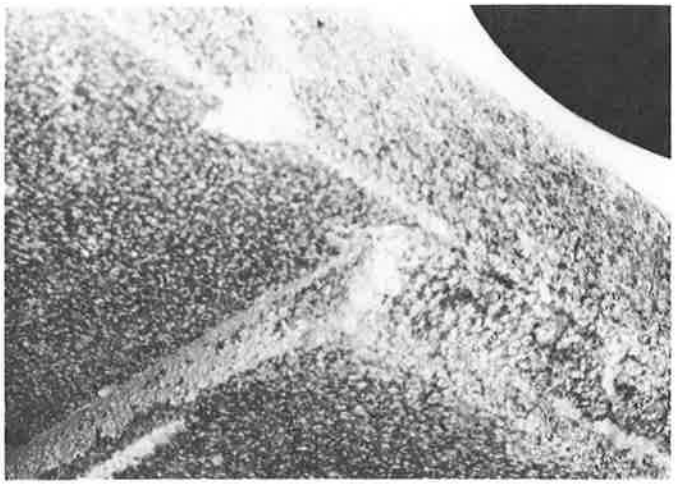

Figure 9 Corrosion Pitting of Beam Flange and Welded Coverplate

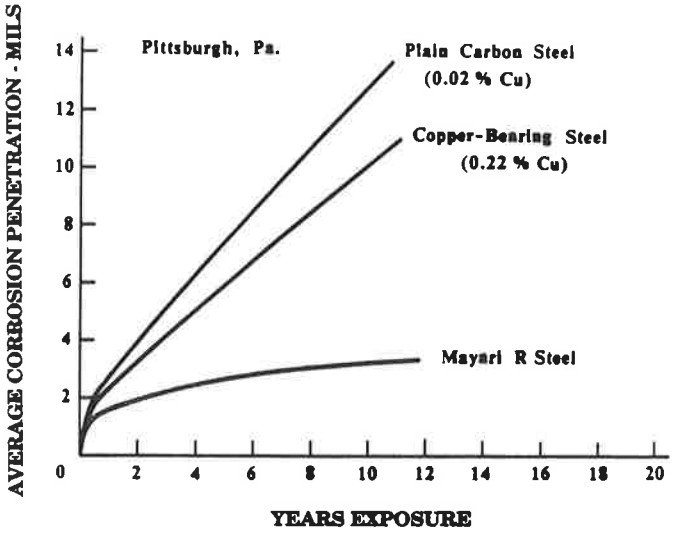

Figure 10 Corrosion of Steels in Industrial Atmosphere

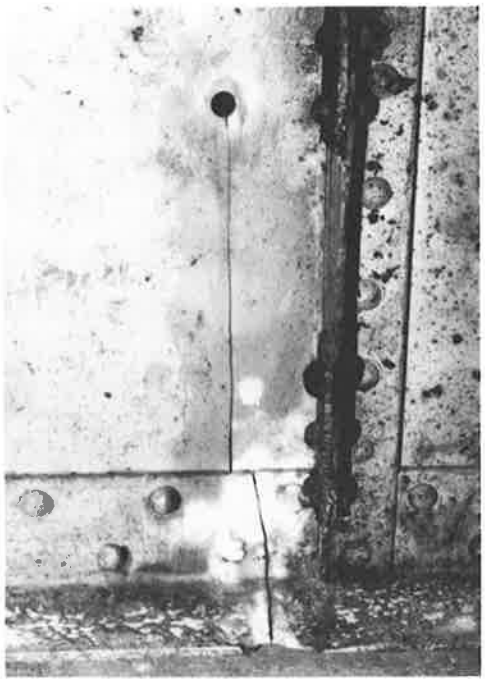

Figure 11 Cracked Components in Corrosion Notched Member

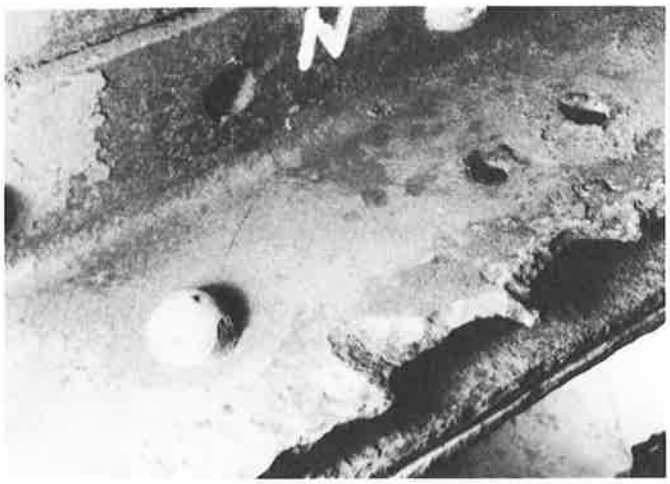

Figure 12 Extensive Corrosion Loss of Tension Flange

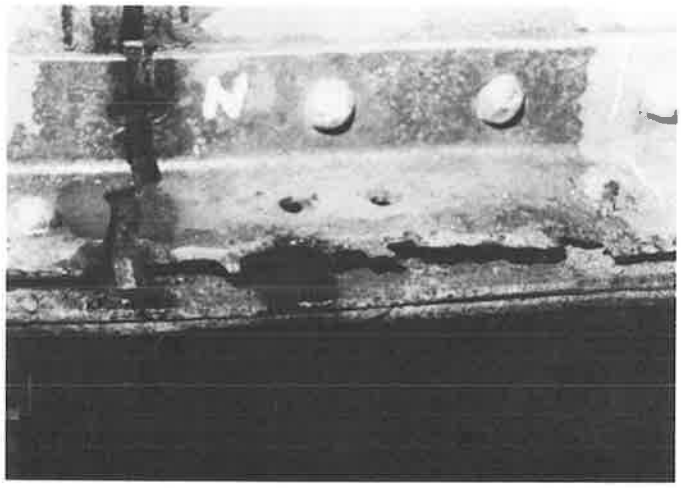

Figure 13 Fatigue Crack Initiated From Corroded Flange Angle

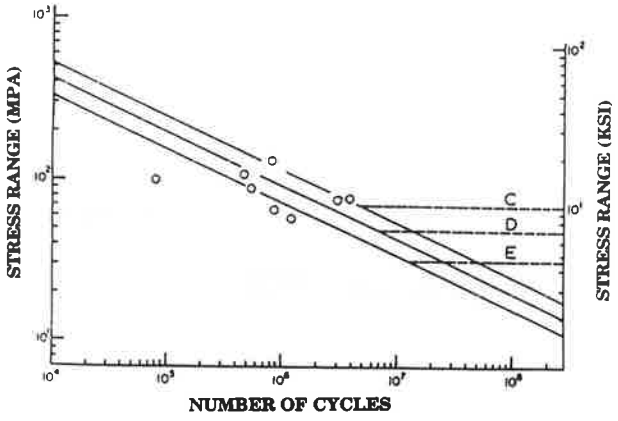

Figure 14 Fatigue Strength of Corrosion Reduced Element

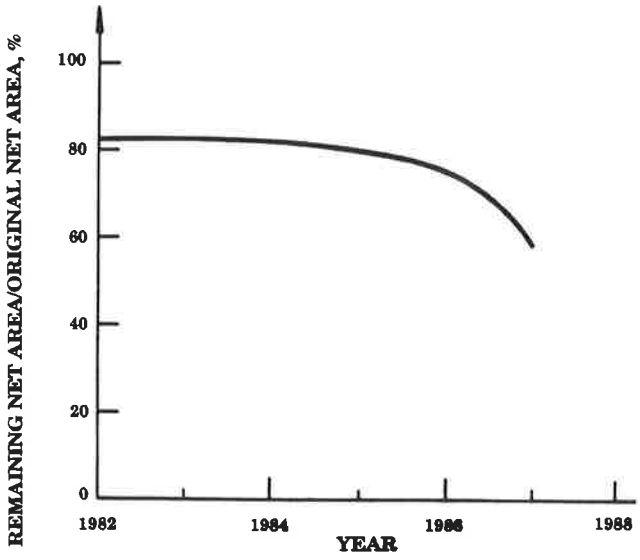

Figure 15 Ratio (%) of Remaining Net Area to Original Net Area as Function of Exposure Time

Figure 16 Corroded Hanger Specimen with Bolted End Fixtures

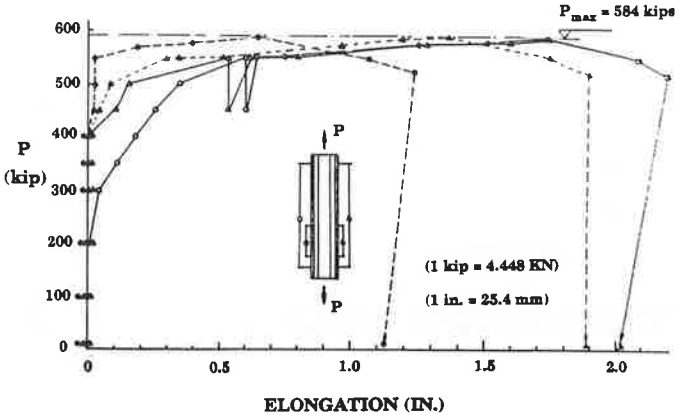

Figure 17 Load-Displacement Relationship of Hanger No. 2

Figure 18 Crack in Flange of Hanger No. 1

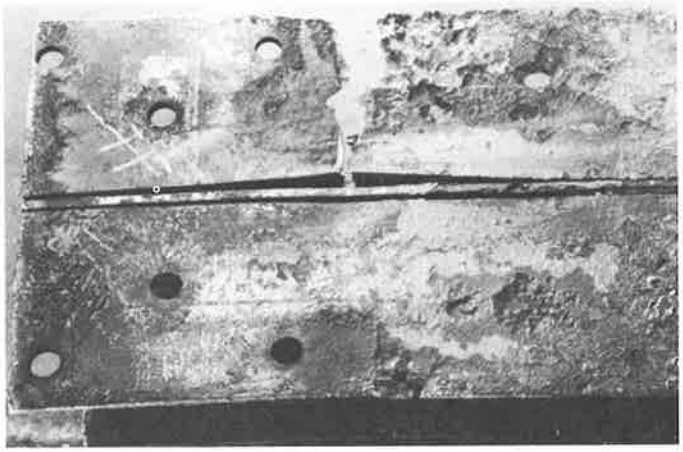

Figure 19 Crack in Flange of Hanger No. 2

Cross-section of Hanger No. 1

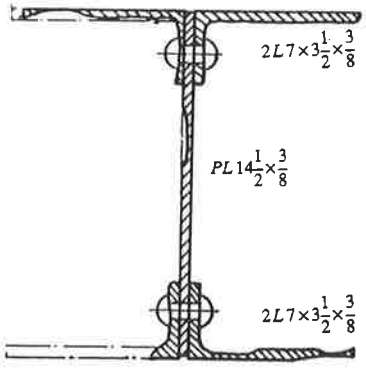

$A_g = 20.6\ in.^2$
$A_n = 18.4\ in.^2$
$A_{nm} = 11.3\ in.^2$

Cross-section of Hanger No. 2

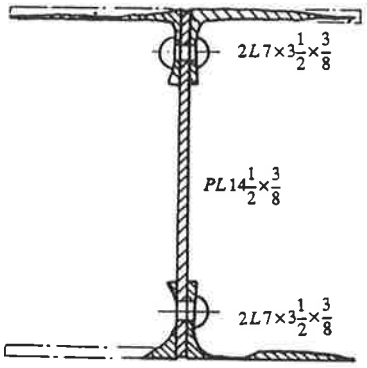

$A_g = 20.6\ in.^2$
$A_n = 18.4\ in.^2$
$A_{nm} = 10.8\ in.^2$

Fig. 20 Remaining Cross-Sectional Area